Influence of Molecular Organization of Ionic Liquids on Electrochemical Properties

by Natalia Borisenko, Rob Atkin, and Frank Endres

Ionic liquids (ILs) are pure salts with melting points typically less than 100°C. ILs exhibit several advantages over conventional molecular liquids in disparate applications because of their remarkable physical properties, which include wide electrochemical stability windows, high ionic conductivity and negligible vapor pressure. IL applications, either already realized or currently under development, encompass many diverse areas such as analytics, catalysis, chemical synthesis, separation technologies, electrochemistry, capacitors, batteries, fuel cells, solar cells, and tribology. Many of these applications involve reactions at the IL/solid interface. Hence, a detailed understanding of the structure of this interface is important and cannot be overstated.

ILs exhibit behavior that is very different from common molecular liquids. As ILs are composed entirely of charged species, they usually exhibit a more pronounced structure in the bulk and at surfaces than molecular liquids.[1] ILs are subject to a range of cohesive interactions (Coulombic, van der Waals, hydrogen bonding and solvophobic forces), resulting in a well-defined nanostructure both in the bulk and at interfaces.[2] The nanostructure of ILs evolves as a consequence of electrostatic interactions between charged groups that produce polar domains. Cation alkyl chains are solvophobically repelled[3] from these charged domains and cluster together to form apolar regions, that in turn produce a sponge-like phase-separated nanostructure.[4] This sponge-like structure present in the bulk changes immediately adjacent to a smooth solid surface. Atomic force microscopy (AFM) force curves[5,6] and reflectivity experiments[7] both reveal the formation of discrete ion or ion pair layers immediately adjacent to the solid surface. This layered surface structure decays to the bulk sponge morphology over a length-scale of a few nanometers.[8]

The IL/solid interface has been the subject of extensive experimental and theoretical studies. Various spectroscopic and scattering methods have been applied to examine this interface.[7,9-21] Electrochemical impedance spectroscopy (EIS) measurements have been used to study the structure and dynamics of ILs.[22-24] Theoretical descriptions of the IL/electrode interface using molecular dynamics and Monte Carlo simulations,[25-35] and mean field theory,[36,37] have predicted "bell-" and "camel-" shaped capacitance curves and oscillating ion density profiles at the electrode surface, consistent with experimental results. However, a proper theoretical model of the electrified IL/solid interface does not yet exist and further experimental studies are required for better understanding the IL/electrode interfacial structure.

During the last decade, *in situ* atomic force microscopy (AFM) and scanning tunneling microscopy (STM) have been extensively used to probe the IL structure at the IL/solid interface.[1,5,8,38-50] The mechanism of operation of the AFM experiment is presented schematically in Fig. 1. The solid electrode substrate and the AFM tip and cantilever are completely immersed within the IL (Fig. 1a). The layers close to the surface are shown schematically as single (blue) layers. As the AFM tip moves towards the surface, it is deflected away due to the forces imparted by the interfacial IL layers. The tip deflection is transformed to a normal force (F) by via Hooke's Law, using the cantilever spring constant. As the tip moves towards the surface, it encounters the first layer (at $d3$). The force experienced increases as the tip pushes against this layer, until sufficient force is reached to rupture the layer (Fig. 1a, blue curve). The tip then jumps into contact with the next layer (at $d2$) and the process is repeated until the tip reaches the innermost layer (at $d1$). The force now increases markedly because the structuring in the innermost layer is the most robust due to the attractive interactions between the IL ions and the surface. When the tip pushes through this layer, it comes into contact with either the substrate surface or a layer of ions that are so strongly bound to the substrate that the tip cannot displace it. The positions of the steps in the force curve are related to the separation (or spatial distribution) of the layers near the surface. The retraction curve can look quite different (Fig. 1a, red curve), most likely either due to attractive interactions between the tip and the surface or interfacial layers, or due to fluid dynamics effects.

(continued on next page)

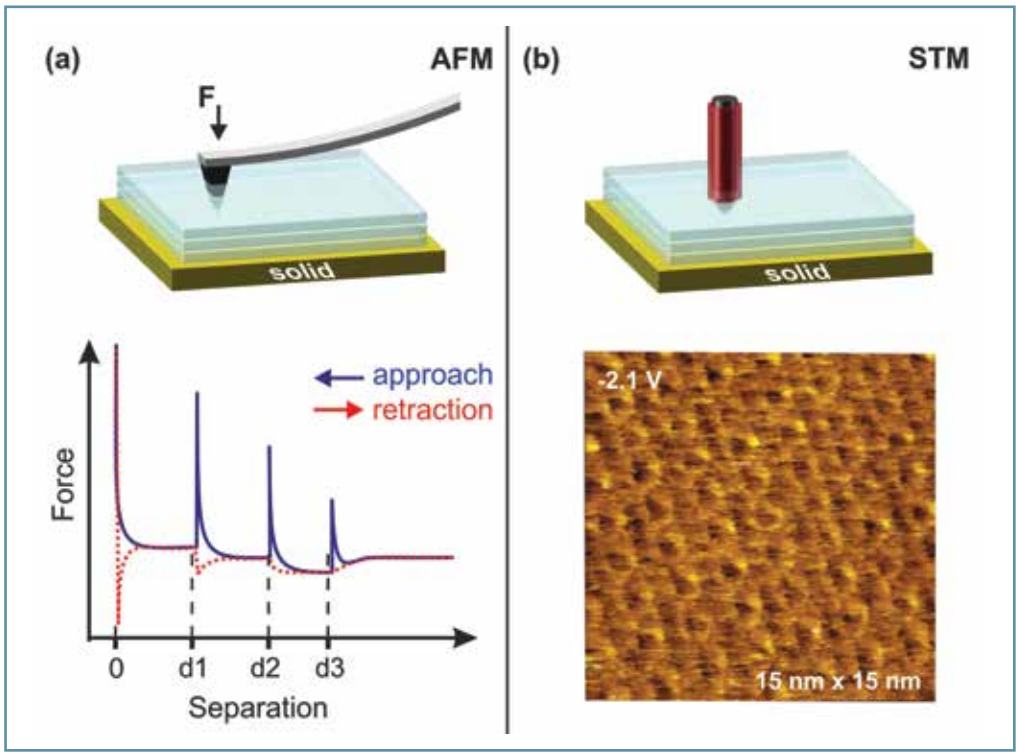

Fig. 1. *(a) Schematic view of an AFM tip approaching a solid surface in the presence of IL with the corresponding force versus distance profile below. (b) Schematic view of a STM tip probing the solid surface immersed within an IL and the real STM-image recorded.*

In the (*in situ*) electrochemical STM experiment, the surface and the STM tip are immersed in the IL (Fig. 1b). The typical distance between the STM tip and the surface is about 1 nm, implying that there is at least one layer between the tip and the sample. The IL ions adsorbed onto the surface participate in the tunneling process, and the STM tip must move through these adsorbed layers during the scanning process. The STM tip either pushes away the layers that are not strongly adsorbed or images them (Fig. 1b).

From AFM results, one can conclude that ILs are strongly adsorbed onto solid surfaces and that several IL layers are present adjacent to the surface.[1,5,6,8,39-41,51] The distance between the layers is the same as the size of an ion pair. The strength of interactions between the innermost layer and the substrate is dependent on the surface, cation and anion type.[6,39] Ion arrangements vary significantly as a function of applied potential, with more pronounced surface structure detected at more positive or more negative potentials. The interfacial layer is enriched by counter-ions strongly bound to the surface. Such strong, specific adsorption will influence electrochemical reactions occurring at the surface.[52]

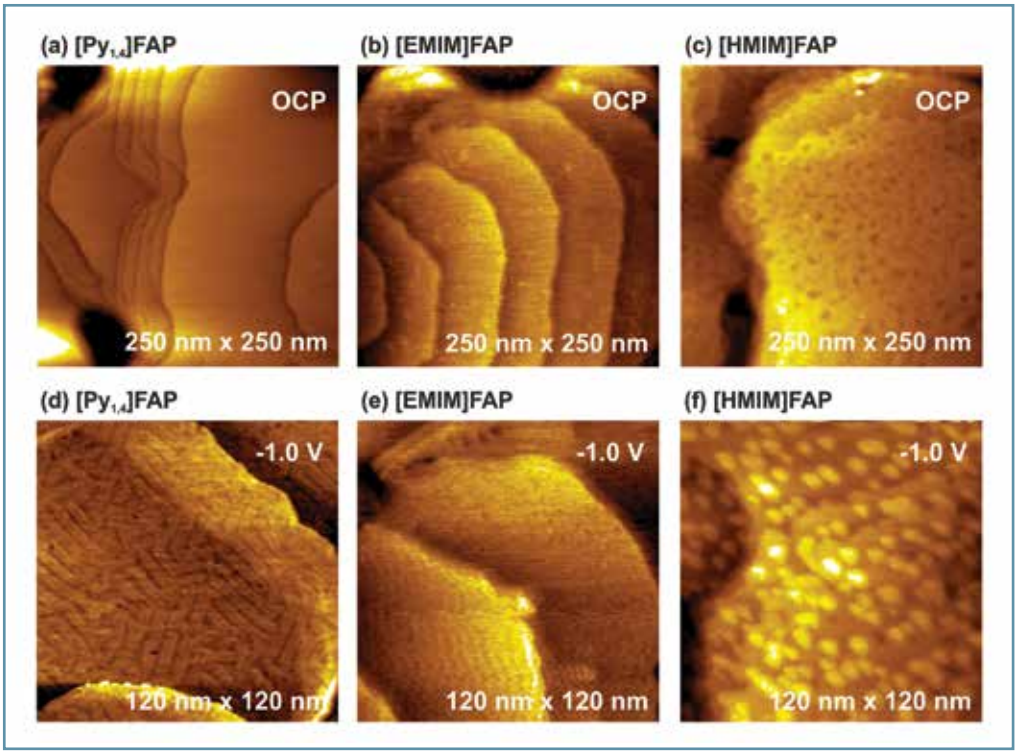

Fig. 2. *(a, d)* In situ *STM images of the Au(111) surface in [$Py_{1,4}$]FAP, (b, e) [EMIM]FAP, and (c, f) [HMIM]FAP.*

In situ STM experiments confirm that ILs adsorbed at an electrode surface do influence electrochemical processes. However, the underlying mechanisms are not yet fully understood. A potential-dependent long-range reconstruction of electrode surfaces has been clearly elucidated, along with the formation of anion/cation adsorption layers at the electrode surface.[8,38,40,43-49,53]

The strong influence of the cation on the IL/electrode interface structure can be clearly seen from *in situ* STM and AFM results obtained for ILs with the tris(pentafluoroethyl)trifluorophosphate (FAP) anion and 3 different cations, namely 1-butyl-1-methylpyrrolidinium ($[Py_{1,4}]^+$), 1-ethyl-3-methylimidazolium ($[EMIM]^+$) and 1-hexyl-3-methylimidazolium ($[HMIM]^+$).[8,38,54] *In situ* STM images show that the appearance of the Au(111) surface differs for each IL (Fig. 2). In the case of [$Py_{1,4}$]FAP, the Au(111) surface is subjected to a restructuring / reconstruction.[8] At the open circuit potential (OCP) (-0.2 V vs. Pt) the typical Au(111) surface is obtained (Fig. 2a). However, in the cathodic regime, the Au(111) surface undergoes a (22 x √3) surface reconstruction leading to a herringbone superstructure (Fig. 2d). The AFM measurements reveal that at the OCP, at least 4 IL layers are present at the interface (Fig. 3a). A small (0.35 nm) step closest to the surface is consistent with an innermost layer enriched in $[Py_{1,4}]^+$. The next spacing (0.9 nm) is consistent with the size of the [$Py_{1,4}$]FAP ion pair dimension. Furthermore, at -1.0 V the width of the ion layer in contact with the gold becomes thinner (0.25 nm in Fig. 3d), indicating that the cation adopts an orientation that renders it more parallel to the surface, which in turn induces the Au(111) (22 x √3) reconstruction (seen in Fig. 2d).

In the case of [EMIM]FAP, the formation of an interaction ion "layer" at the OCP (-0.2 V vs. Pt) results in unclear images (Fig. 2b). The roughness of this "layer" increases at more negative electrode potentials (Fig. 2e).[54] Two small steps, 0.3 nm and 0.5 nm wide, are detected that likely correspond to cation (0.3 nm) and anion (0.5 nm) sublayers (Fig. 3b). Their sum (0.3 nm + 0.5 nm) gives the [EMIM] FAP ion pair dimension (0.83 nm).[39] At a potential of -1.0 V, instead of an anion layer adsorbed at the surface, an ion-pair sized step is detected in the second layer (Fig. 3e).

Both *in situ* STM and AFM results show that multiple ionic liquid interfacial layers form at the Au(111) electrode interface in [HMIM]FAP.[38] At the OCP (-0.05 V vs. Pt) the STM images show a wormlike surface structure with ~0.3 nm deep vacancies (Fig. 2c). The AFM data reveals a weakly bound, cation-rich interfacial layer covered by an anion rich layer (Fig. 3c). If the electrode potential is reduced to -1.0 V, islands of *ca.* 0.2-0.4 nm in height (which correlates well with the size of the cation) can be observed (Fig. 2f). At a potential of -1.0 V, an ion pair sized step is detected in the second layer, as opposed to an anion sized step (Fig. 3f).

These *in situ* STM and AFM results show that the IL cation has a strong influence on the structure and composition of the interface. With the same anion, the Au(111) surface undergoes the (22 x √3) reconstruction with $[Py_{1,4}]^+$, but with $[EMIM]^+$ and $[HMIM]^+$ the herringbone superstructure is not obtained. This can perhaps be due to specific cation/surface, cation/anion and cation/cation interactions, which are strongly dependent on the type of the functional groups (pyrrolidinium or imidazolium ring and the length of the alkyl chains), and therefore will be different for various cations. It is likely that the different cations have different orientations in the interfacial layer depending on their chemical structure and the applied electrode potential. This in turn induces different surface structures (c.f. Fig. 2). Thus, a particular geometrical configuration of $[Py_{1,4}]^+$ at a potential of -1.0 V causes the Au(111) (22 x √3) reconstruction shown in Fig. 2d, while $[EMIM]^+$ and $[HMIM]^+$ do not seem to favor the herringbone superstructure.

Solutes dissolved in ionic liquids also influence their interfacial structure. For instance, AFM experiments reveal that interfacial layering is markedly weaker when LiCl in added to an IL[43,55] and *in situ* STM measurements show that, unlike for the pure IL (Fig. 4a), the "reconstruction" of the gold surface is different in the presence of LiCl

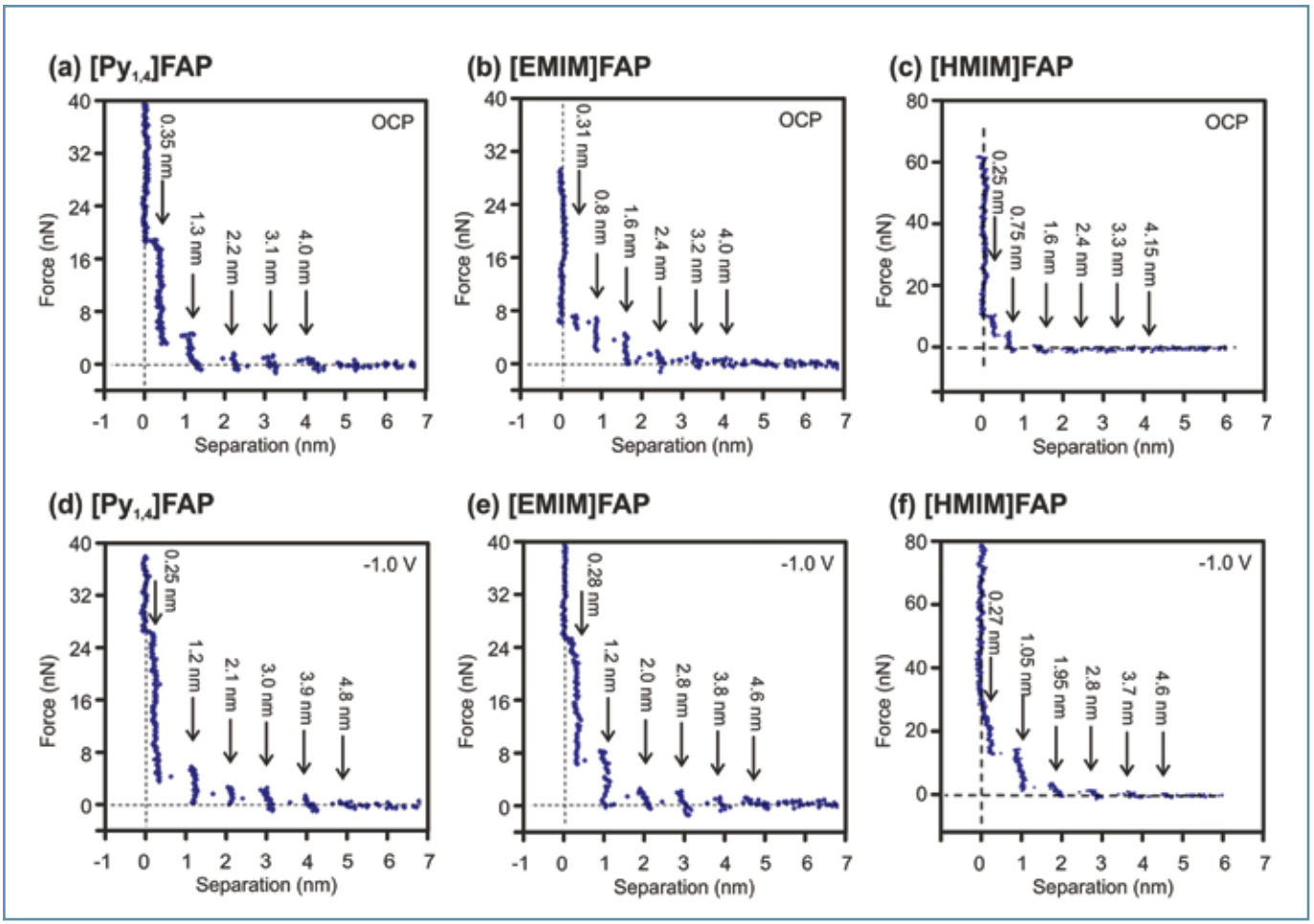

Fig. 3. *(a, d) Typical force versus distance profile for an AFM tip approaching a Au(111) surface in [$Py_{1,4}$]FAP, (b, e) [EMIM]FAP, and (c, f) [HMIM]FAP.*

(Fig. 4b). At negative electrode potentials, both $[Py_{1,4}]^+$ and Li^+ ions will interact with the gold surface. Therefore, at a potential of -1.2 V, the adsorption of the $[Py_{1,4}]^+$ will induce the Au(111) (22 x √3) reconstruction, while the adsorption of Li^+ will reduce the interfacial structure hindering the (22 x √3) reconstruction. These two competing effects will lead to the structure presented in Fig. 4b, where Au(111) undergoes an incomplete herringbone reconstruction.

Outlook

Ionic liquids exhibit a remarkably diverse interfacial chemistry, with multiple interfacial layers present at the IL/solid interface. The adsorption strength of ILs onto solid surfaces is much higher than for typical organic solvents or water. The structure and composition of the interfacial layer can be tuned by varying the surface potential and the ionic structure, and by addition of solutes. This allows us to envision that IL interfacial properties can be readily matched to a particular application once the required fundamental understanding is elucidated. Further studies of the IL/electrode interface, both in pure ILs, and in the presence of solutes, are required to fulfil this vision.

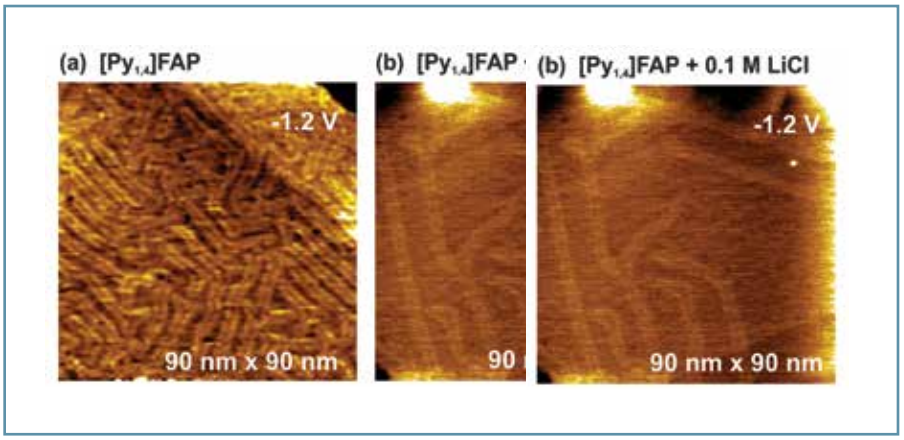

Fig. 4. In situ *STM images of the Au(111) surface in (a) [$Py_{1,4}$]FAP and (b) [$Py_{1,4}$]FAP containing 0.1 M LiCl.*

About the Authors

Natalia Borisenko studied electrochemistry and physical chemistry at the St. Petersburg State Polytechnical University (St. Petersburg, Russia) from 1997-2003 and got her Masters degree there in 2003. In the same year she joined the group of Endres (Clausthal University of Technology, Clausthal, Germany) where she obtained her Dr. rer. nat (PhD) degree in 2006. Currently she is working at the same university in the group of Prof. Endres. Her main interests cover the electrochemistry of ionic liquids, the processes at the ionic liquid / solid interfaces, and the electrodeposition of

(continued on next page)

(continued from previous page)

metals and semiconductors from ionic liquids. She may be reached at natalia.borissenko@tu-clausthal.de.

Rob Atkin is an Australian Research Council Future Fellow and Associate Professor at the University of Newcastle, Australia. After completing a PhD in 2003 focused on the mechanism of surfactant adsorption at the solid liquid interface, he completed postdoctoral work at Bristol University (UK) in Brian Vincent's laboratory studying micro-encapsulation. In 2005 he was awarded an Australian Research Council Postdoctoral Fellowship to study surfactant self-assembly in ionic liquids at the University of Sydney, then in 2007 he received a University of Newcastle Research Fellowship. His research is centered on bulk and interfacial ionic liquid structure, and associated properties, and he leads the Newcastle Ionic Liquid group. He may be reached at rob.atkin@newcastle.edu.au.

Frank Endres studied chemistry at the Saarland University (Saarbrucken, Germany) from 1988-1993 and graduated there in 1993 with a diploma in Chemistry. He got his Dr. rer. nat. (PhD) degree in 1996 at the same university and moved subsequently to the university of Karlsruhe where he got his habilitation for physical chemistry in 2002. In the same year he was appointed by the Clausthal University of Technology as Professor and became in 2012 the founding director of the new Institute of Electrochemistry there. His interests comprise the physical chemistry of surfaces and interfaces, ionic liquid electrochemistry and materials science. He may be reached at frank.endres@tu-clausthal.de.

References

1. R. Hayes, G. G. Warr, and R. Atkin, *Phys. Chem. Chem. Phys.* **12**, 1709 (2010).
2. R. Hayes, S. Imberti, G. G. Warr, and R. Atkin, *Phys. Chem. Chem. Phys.*, **13**, 3237 (2011).
3. A. Ray, *Nature*, **231**, 313 (1971).
4. R. Atkin, and G. G. Warr, *J. Phys. Chem. B*, **112**, 4164 (2008).
5. R. Atkin, and G. G. Warr, *J. Phys. Chem. C*, **111**, 5162 (2007).
6. H. Li, F. Endres, and R. Atkin, *Phys. Chem. Chem. Phys.*, **15**, 14624 (2013).
7. M. Mezger, S. Schramm, H. Schroder, H. Reichert, M. Deutsch, E. J. De Souza, J. S. Okasinski, B. M. Ocko, V. Honkimaki, and H. Dosch, *J. Chem. Phys.*, **131**, 094701 (2009).
8. R. Atkin, N. Borisenko, M. Drüschler, S. Zein El Abedin, F. Endres, R. Hayes, B. Huber, and B. Roling, *Phys. Chem. Chem. Phys.*, **13**, 6849 (2011).
9. A. J. Carmichael, C. Hardacre, J. D. Holbrey, M. Nieuwenhuyzen, and K. R. Seddon, *Mol. Phys.*, **99**, 795 (2001).
10. Y. Jeon, J. Sung, W. Bu, D. Vaknin, Y. Ouchi, and D. Kim, *J. Phys. Chem. C*, **112**, 19649 (2008).
11. E. Sloutskin, B. M. Ocko, L. Tamam, I. Kuzmenko, T. Gog, and M. Deutsch, *J. Am. Chem. Soc.*, **127**, 7796 (2005).
12. M. Mezger, H. Schröder, H. Reichert, S. Schramm, J. S. Okasinski, S. Schöder, V. Honkimäki, M. Deutsch, B. M. Ocko, J. Ralston, M. Rohwerder, M. Stratmann, and H. Dosch, *Science*, **322**, 424 (2008).
13. J. Bowers, M. C. Vergara-Gutierrez, and J. R. P. Webster, *Langmuir*, **20**, 309 (2003).
14. J. B. Rollins, B. D. Fitchett, and J. C. Conboy, *J. Phys. Chem. B*, **111**, 4990 (2007).
15. B. D. Fitchett, and J. C. Conboy, *J. Phys. Chem. B*, **108**, 20255 (2004).
16. S. Baldelli, *Acc. Chem. Res.*, **41**, 421 (2008).
17. C. Aliaga, and S. Baldelli, *J. Phys. Chem. B*, **110**, 18481 (2006).
18. C. Aliaga, and S. Baldelli, *J. Phys. Chem. C*, **112**, 3064 (2008).
19. C. Romero, H. J. Moore, T. R. Lee, and S. Baldelli, *J. Phys. Chem. C*, **111**, 240 (2006).
20. T. Cremer, M. Stark, A. Deyko, H. P. Steinrück, and F. Maier, *Langmuir*, **27**, 3662 (2011).
21. T. Cremer, L. Wibmer, S. K. Calderon, A. Deyko, F. Maier, and H. P. Steinrück, *Phys. Chem. Chem. Phys.*, **14**, 5153 (2012).
22. V. Lockett, R. Sedev, J. Ralston, M. Horne, and T. Rodopoulos, *J. Phys. Chem. C*, **112**, 7486 (2008).
23. T. R. Gore, T. Bond, W. Zhang, R. W. J. Scott, and I. J. Burgess, *Electrochem. Commun.*, **12**, 1340 (2010).
24. V. Lockett, M. Horne, R. Sedev, T. Rodopoulos, and J. Ralston, *Phys. Chem. Chem. Phys.*, **12**, 12499 (2010).
25. M. V. Fedorov, N. Georgi, and A. A. Kornyshev, *Electrochem. Commun.*, **12**, 296 (2010).
26. J. Vatamanu, O. Borodin, and G. D. Smith, *J. Am. Chem. Soc.*, **132**, 14825 (2010).
27. J. Vatamanu, O. Borodin, and G. D. Smith, *J. Phys. Chem. B*, **115**, 3073 (2011).
28. S. A. Kislenko, I. S. Samoylov, and R. H. Amirov, *Phys. Chem. Chem. Phys.*, **11**, 5584 (2009).
29. S. K. Reed, O. J. Lanning, and P. A. Madden, *J. Chem. Phys.*, **126**, 084704 (2007).
30. M. V. Fedorov, and A. A. Kornyshev, *J. Phys. Chem. B*, **112**, 11868 (2008).
31. M. V. Fedorov, and A. A. Kornyshev, *Electrochim. Acta*, **53**, 6835 (2008).
32. G. Feng, J. S. Zhang, and R. Qiao, *J. Phys. Chem. C*, **113**, 4549 (2009).
33. S. Wang, S. Li, Z. Cao, and T. Yan, *J. Phys. Chem. C*, **114**, 990 (2009).
34. N. Georgi, A. A. Kornyshev, and M. V. Fedorov, *J. Electroanal. Chem.*, **649**, 261 (2010).
35. A. I. Frolov, K. Kirchner, T. Kirchner, and M. V. Fedorov, *Faraday Discuss.*, **154**, 235 (2012).
36. A. A. Kornyshev, *J. Phys. Chem. B*, **111**, 5545 (2007).
37. K. B. Oldham, *J. Electroanal. Chem.*, **613**, 131 (2008).
38. T. Carstens, R. Hayes, S. Zein El Abedin, B. Corr, G. B. Webber, N. Borisenko, R. Atkin, and F. Endres, *Electrochim. Acta*, **82**, 48 (2012).
39. R. Hayes, N. Borisenko, M. K. Tam, P. C. Howlett, F. Endres, and R. Atkin, *J. Phys. Chem. C*, **115**, 6855 (2011).
40. R. Atkin, S. Zein El Abedin, R. Hayes, L. H. S. Gasparotto, N. Borisenko, and F. Endres, *J. Phys. Chem. C*, **113**, 13266 (2009).
41. R. Hayes, S. Zein El Abedin, and R. Atkin, *J. Phys. Chem. B*, **113**, 7049 (2009).
42. D. Wakeham, R. Hayes, G. G. Warr, and R. Atkin, *J. Phys. Chem. B*, **113**, 5961 (2009).
43. F. Endres, N. Borisenko, S. Zein El Abedin, R. Hayes, and R. Atkin, *Faraday Discuss.*, **154**, 221 (2012).
44. L. G. Lin, Y. Wang, J. W. Yan, Y. Z. Yuan, J. Xiang, and B. W. Mao, *Electrochem. Commun.*, **5**, 995 (2003).
45. Y.-Z. Su, Y.-C. Fu, J.-W. Yan, Z.-B. Chen, and B.-W. Mao, *Angew. Chem.*, Int. Ed. **48**, 5148 (2009).
46. G.-B. Pan, and W. Freyland, *Chem. Phys. Lett.*, **427**, 96 (2006).
47. Y.-Z. Su, J.-W. Yan, M.-G. Li, Z.-X. Xie, B.-W. Mao, and Z.-Q. Tian, *Z. Phys. Chem.*, **226**, 979 (2012).
48. M. Gnahm, T. Pajkossy, and D. M. Kolb, *Electrochim. Acta*, **55**, 6212 (2010).

49. F. Endres, S. Zein El Abedin, and N. Borissenko, *Z. Phys. Chem.*, **220**, 1377 (2006).
50. J. J. Segura, A. Elbourne, E. J. Wanless, G. G. Warr, K. Voitchovsky, and R. Atkin, *Phys. Chem. Chem. Phys.*, **15**, 3320 (2013).
51. H. Li, M. W. Rutland, and R. Atkin, *Phys. Chem. Chem. Phys.*, **15**, 14616 (2013).
52. F. Endres, O. Höfft, N. Borisenko, L. H. Gasparotto, A. Prowald, R. Al-Salman, T. Carstens, R. Atkin, A. Bund, and S. Zein El Abedin, *Phys. Chem. Chem. Phys.*, **12**, 1724 (2010).
53. M. Gnahm, C. Berger, M. Arkhipova, H. Kunkel, T. Pajkossy, G. Maas, and D. M. Kolb, *Phys. Chem. Chem. Phys.*, **14**, 10647 (2012).
54. N. Borisenko, S. Zein El Abedin, and F. Endres, *ChemPhysChem*, **13**, 1736 (2012).
55. R. Hayes, N. Borisenko, B. Corr, G. B. Webber, F. Endres, and R. Atkin, *Chem. Commun.*, **48**, 10246 (2012).